Neuroinform
DOI 10.1007/s12021-007-9007-5

Higher Derivatives of ERP Responses to Cross-Modality Processing

Jean-Philippe Thivierge

Received: 7 September 2007 / Accepted: 11 December 2007

Abstract Determining the links between cognitive processes and neuroelectrical brain activity (i.e., event-related potentials, ERPs) depends strongly on our understanding of how this activity fluctuates in response to stimuli; however, the way in which changes in ERP amplitudes can accelerate and decelerate over time has received only scant attention. The present study demonstrates that moment-to-moment changes (i.e., derivatives) of ERP responses convey information that is not readily accessible from the amplitude of response. Subjects exposed to visual and auditory stimuli either alone (unimodal) or combined (crossmodal) yielded different responses according to particular derivatives of ERP activation. In particular, an effect of cross-modality integration (stronger activation for crossmodal compared to unimodal stimuli) was detected in the higher derivatives of activation of a number of electrode sites spanning a fronto-centro-parietal distribution; in most sites, no such effect was detected in the amplitude of waveforms itself. These results suggest that information may be carried by the higher derivatives of ERP responses, and that distinct topographic distributions are associated with different derivatives of response. These different derivatives of response may in turn relate to different strategies for sensory processing in the brain, and in particular reflect a fundamental mode of information processing by time derivatives previously reported in cortex.

Electronic supplementary material The online version of this article (doi:10.1007/s12021-007-9007-5) contains supplementary material, which is available to authorized users.

J.-P. Thivierge (✉)
Department of Psychological and Brain Sciences,
Indiana University,
1101 East Tenth Street,
Bloomington, IN 47405, USA
e-mail: jthivier@indiana.edu

Keywords Event-related brain potentials · Cross-modality integration · Functional data analysis

Introduction

A primary goal of experiments on event-related potentials (ERPs) is to relate time-domain changes in brain activity to particular aspects of cognitive and behavioral information processing in the brain (Lopes da Silva 1999; Picton 1988). But as several authors have made clear, the information contained in brain activity depends not only on the amplitude of signals over time, but also on the speed (i.e., first derivative) at which these changes occur (Freeman et al. 2006). This observation raises important questions pertaining to the particular conditions under which modulations in first derivative occur, as well as, ultimately, their functional significance for neural information processing. These questions have received only scant attention, and certainly merit further consideration.

The central theme of this paper can be formulated as follows: is it possible to extract information contained in the moment-to-moment changes in first (or higher) derivatives of ERPs that cannot be readily found when analyzing raw amplitudes? On the one hand, derivatives may not convey any extra information over what is already present in the amplitude of ERPs. The wealth of information already collected in the amplitude of ERPs with respect to particular cognitive demands might suggest that, in fact, fluctuations in amplitude carry all of the information to be gained from ERPs; variations in first (and possibly higher) derivatives could be a mere "artifact" of these fluctuations, conveying no unique insights on neural information processing.

On the other hand, differences in derivatives across experimental conditions may reflect aspects of ERPs that

are not readily accessible when examining differences in amplitude. For instance, this may happen in a case where two waveforms differ in the speed at which changes in amplitude occur (e.g., sharp vs. more gradual changes), yet reach a similar peak amplitude at a similar time. While the overall duration of a peak may differ between these two waveforms, this measure is not necessarily precise enough to describe moment-to-moment changes in amplitude within a particular peak. Leaving possible functional consequences aside for the moment (see "Discussion"), it is straightforward that reliable differences in the peaks of the first derivative across experimental conditions may occur even in the absence of differences in peak amplitudes and latencies.

The current paper aims to test whether such a scenario arises experimentally, and whether information may be contained in the first, second, and third derivatives of ERP responses. As with the first derivative, reliable (i.e., consistent across trials and subjects) aspects of neural information processing may be uniquely identifiable in these higher derivatives.

The present study considers a task that includes both unimodal (visual or auditory) and crossmodal (both visual and auditory) stimuli. According to a wealth of evidence, crossmodal stimuli lead to faster response times for object identification, and generate stronger amplitudes of evoked N100 responses, potentially reflecting the integration of information across different sensory modalities at an early stage of visual processing (i.e., *cross-modality integration*; Fort et al. 2002; Giard and Peronnet 1999; Molholm et al. 2004; Teder-Salejarvi et al. 2005). However, prior work has not examined higher derivatives of responses; here it is argued that these higher derivatives may convey information about neural processing that is not readily accessible from inspecting the latency and peak amplitude of waveforms.

In order to test this hypothesis, derivatives of ERP responses are computed through Functional Data Analysis (FDA; Ramsay and Silverman 2005), an approach of widespread use in signal processing, and beginning to be applied to ERPs (Thivierge 2007). Essentially, FDA allows the computation of higher derivatives of ERP responses through the approximation of waveforms by B-spline functions. Importantly, FDA can be used to analyze moment-to-moment changes in the first (or higher) derivatives in order to precisely determine at what point in time (following stimulus onset) two experimental conditions begin to diverge.

The remainder of this paper is structured as follows. First, the experimental procedure is described, along with an overview of the main steps involved in applying FDA to ERPs. Then, behavioral results examining the effects of cross-modality and congruency on response times and accuracy are provided. Third, the results of FDA analyses are reported, examining both integration (unimodal vs crossmodal conditions) and congruency effects (crossmodal conditions where the information agreed vs did not agree, e.g., a barking dog vs a meowing dog) at different points in time following stimulus onset. Finally, the Discussion addresses the possible functional links between higher derivatives of ERP responses and neural information processing, and raises some implications for future work on functional connectivity.

Methods

Experimental Methods

Participants Fifteen young adults with normal hearing and normal or corrected-to-normal vision took part in this study. Two of the participants were excluded due to poor behavioral performances (reaction times greater than two standard deviations above the mean). The final sample was thus composed of 12 individuals (6 men), between the ages of 18 and 33 (mean age: 25.1±3.8 years). Following approval by Concordia University's research ethics board, all participants were recruited from a subject pool in the Department of Psychology (Concordia University, Montreal, Canada). Informed consent was obtained from each participant prior to testing.

Stimuli Both auditory and visual stimuli were employed. The visual stimuli consisted of 12 Gaussian-blurred grey-scale photographs of animals (see Supplementary Material, Fig. S1) of size 10×10 cm. Stimuli were presented at a visual angle of 8.3° on a 16.1″ CRT monitor.

The auditory stimuli consisted of animal vocalization sounds (e.g., a cow "moo") selected from various online sound effect libraries. Samples (11025 Hz, 8 bit) were presented binaurally at 75 dB SPL using tube ear inserts (Neuroscan, El Paso, TX,USA), with a stimulus onset asynchrony of 2.5 s, and a stimulus duration of 600 ms. Stimulus presentation was controlled via Gentask software (NeuroScan, version 2.4.18).

Experimental protocol Four distinct experimental conditions were devised, where either auditory stimuli alone (auditory condition), visual stimuli alone (visual condition), conflicting auditory and visual stimuli (i.e., representing different animals, crossmodal incongruent), and congruent stimuli (i.e., representing the same animal, crossmodal congruent) were presented. In the two audio-visual (AV) conditions, the visual and auditory stimuli were presented simultaneously. A total of 180 trials for each of these conditions were presented in a random fashion.

In the auditory and visual conditions, participants were required to categorize animals as either "large" or "small" ("small" was defined as being small enough to fit under the

chair that the participant was sitting on); in the two AV conditions, participants had to respond based on the auditory stimuli alone. Responses were registered by pressing the left or right buttons (counterbalanced across participants) on a response box (Neuroscan, El Paso, TX, USA). The maximum allowed response time was 2 s following stimulus onset.

The same number of large and small animals was used as stimuli (both visual and auditory). No statistical differences were found between the two groups (large vs. small animals) in terms of mean pixel luminance [independent sample t-test: $t(10)=1.7$, $p>0.12$] and root mean square contrast [$t(10)=-2.1$, $p>0.7$]. In addition, no differences were found between the two groups in terms of both the frequencies associated with the highest dB levels [$t(10)=1.03$; $p>0.33$], and the fundamental frequencies (extracted using the PRAAT software; Boersma and Weenink 2006) [$t(10)=1.17$; $p>0.27$]. In the crossmodal incongruent condition, 95 pairs of stimuli combined different animals from conflicting categories (i.e., one large and one small), and 85 pairs were composed of different animals from the same category. An equal number of trials included the sound of a large animal and that of a small animal.

Electrophysiology A continuous EEG was recorded at 32 tin electrodes mounted in an elastic nylon cap (Electro-Cap International, Inc., Eaton, OH, USA), arranged according to the International 10/20 system using a cephalic (forehead) location as ground, and referenced to linked ear lobes. EEG signals were recorded at a sampling rate of 500 Hz using a DC-100 Hz bandwidth (with electrical impedances kept below 5 kΩ) and amplified using NeuroScan Synamps (Neuroscan, El Paso, TX, USA). Trials with EOG activity (horizontal and vertical eye movements) exceeding ±75 μV were rejected; on average, 16.7% (SD 12.3%) of unisensory (only auditory or visual) trials and 20.4% (SD 13.4%) of multisensory (crossmodal congruent and incongruent) trials were rejected. Offline filtering was performed for frequencies between 1–30 Hz. For all FDA analyses performed, the raw waveforms were averaged across both trials and participants. Then, FDA B-spline fitting was performed using a sampling rate of 500 Hz. Only 22 electrodes where responses were strongest are included in analyses: FP1, FP2, FZ, F3, F4, F7, F8, CZ, C3, C4, PZ, P3, P4, T5, T6, O2, FT8, FT8, CPZ, CP3, CP4, FC3.

Functional Data Analysis

Overview The general goal of FDA is to model a set of raw data samples using continuous functions that can then be analyzed and interpreted. The analysis of ERP signals can be broken down into three distinct steps. First, averages of ERP signals are computed over all trials within each condition, independently for all participants. Second, the resulting raw ERP data are fitted by a temporally continuous function that is smoother (i.e., exhibits fewer fluctuations) than the original data. Third, the first, second, and third-order derivatives of this function are computed. This differs from other work examining the area under the ERP curve (Gibbons and Stahl 2007). According to the fundamental theorem of calculus, the derivative of an integral returns the original function; thus, the two measures are linked but clearly different. A complete description of FDA is available elsewhere (Ramsay and Silverman 2005), and FDA Matlab software can be obtained at: http://www.psych.mcgill.ca/faculty/ramsay/ramsay.html.

B-spline smoothing In FDA analysis, a continuous dependent variable x_j is assumed, representing the amplitude of the electrical signal measured over time—in our case, this is an average waveform over participants, computed separately for each experimental condition. Although time (the independent variable) is continuous, our equipment provides us with samples at discrete time steps t_j, $j=1,...,n$. Sampling is performed at constant time intervals (500 Hz), but this is not required by the model.

Formally, the functional observation $y(t)$ consists of n pairs (t_j, x_j), where x_j is a recording of observations (each indexed j), and t_j is the time at which the sample was taken:

$$x_j = y(t_j) + \varepsilon_j. \tag{1}$$

The error term ε_j describes the noise present in the raw data. FDA converts the sampled data into a *functional form*. Raw data is approximated using a continuous function $y(t)$ over some delimited interval. FDA builds the approximated function as a combination of primitive functions, each termed a *basis*. FDA supports several types of basis functions, and the choice of a particular basis is problem-specific. For ERP signals, B-spline bases were chosen. This basis is commonly used for non-periodic data (i.e., data without any assumed periodicity over time; this is appropriate for qualifying peaks and troughs over a short time-window following stimulus onset, as typically required in ERPs; Basar et al. 1999; Demiralp et al. 2001).

A linear combination of basis functions is used to represent raw data in a functional form. This linear combination approximates the raw data as a smooth function, and reduces noise by avoiding overfitting. Function fitting can be viewed as a trade-off between a perfect fit to the data (that keeps all signal information, but also noise), and a very smooth function (that eliminates noise, but also signal). FDA proposes two techniques for controlling function smoothness: (1) controlling the number of intervals K and (2) roughness penalty (cf. Eqs. 4 and 5 below).

Approximated functions $y(t)$ can be represented as basis function expansions, that is, a linear mixture $\phi_k, k = 1, ..., K$:

$$y(t) = \sum_{k}^{K} c_k \phi_k(t). \quad (2)$$

One of the parameters that controls smoothing is the number K of basis functions. Assuming that an $n \times K$ matrix $\Phi = \{\phi_k(t_j)\}$ of basis function values at the observation points is of full rank, an exact representation is generally possible when $K=n$, in the sense that the coefficients c_k can be chosen to yield $y(t_j) = x_j$ for each j. Once a system of B-spline bases is defined (cf. Eq. 2), an approximated function is obtained by adjusting the coefficients c_k of the expansion, in order to minimize a sum of squared errors (SSE). This criterion computes the distance between the x_j observations on the one hand, and the weighted ϕ bases on the other:

$$\mathrm{SSE}(x|c) = (x - \Phi c)'(x - \Phi c) \quad (3)$$

where the K-vector c contains the coefficients c_k. The precision sought by the minimization of SSE is 0.0001.

Roughness penalty regularization In addition to the number of bases K, FDA can control the smoothness of the approximated function using a penalty term added to the SSE criterion of Eq. 3. This term represents an integrated square derivative:

$$\mathrm{PEN}(y) = \int [\partial^m y(t)/(\partial t)^m]^2 dt. \quad (4)$$

This penalty assesses the total curvature in $y(t)$, equivalent to the degree to which $y(t)$ departs from a straight line. An integral is taken over the entire time window of interest in order to penalize departures from a straight line over the entire range of the function and not simply at a local point in time (Ramsay and Silverman 2005).

The goal of this penalty is to reduce the presence of large values in the mth derivative of a function, resulting in smoother functions. It is recommended to penalize two derivatives higher than the largest derivative of interest (Ramsay and Silverman 2005). For instance, to consider variations in the function itself, the second derivative is penalized.

With the roughness penalty of Eq. 4, the least squares criterion of Eq. 3 is redefined as follows:

$$\mathrm{PENSSE}_\lambda(x|c) = (x - \Phi c)'(x - \Phi c) + \lambda \times \mathrm{PEN}(y), \quad (5)$$

where λ is a parameter that controls the amount of penalty to be applied. The criterion of Eq. 5 can be optimized in linear $O(n)$ time for splines (Green and Silverman 1994). When smooth fitting an ERP waveform based on Eq. 5, one assumption is that noise is of higher frequency than the signal; this assumption is justified given our goal of analyzing ERP components, which represent wide fluctuations in signal, rather than high-frequency "jitter".

Higher values of λ yield a function that is smoother but underfits the data, while lower values yield a function that is rougher but offers a closer fit. Of course, the choice of a particular smoothing parameter (λ) will influence the resulting smooth functions generated. A higher smoothing parameter than the one employed here would eliminate higher derivatives of response; conversely, a lower parameter would increase these higher derivatives. Here, our value was chosen to capture the main components of variation of the ERP waveforms, while reducing some of the "jitter" present originally; an analysis of the influence of smoothing can be found in the Supplementary Material (Fig. S5; see also Thivierge 2007), and demonstrates that, within reasonable limits, different choices of λ will lead to qualitatively comparable results (more sophisticated approaches to optimizing the degree of smoothing have also been proposed, e.g., based on maximum likelihood approaches (Friston et al. 2006).

In summary, the first step in our method involves fitting a series of discrete observations with a continuous function formed with a combination of B-spline bases. The goal of this function is to capture the main characteristics of variation of the raw data. Extra roughness is smoothed out by penalizing higher derivatives of the function so that the approximated curve shows a cognitively plausible number of peaks and troughs.

Topographical distribution of crossmodal integration In order to measure the difference between the amplitude of responses for unimodal and crossmodal stimuli, the positive and negative inflection points are identified. The temporal location of these points (with respect to stimulus onset) is identified by a zero crossing one derivative higher; for instance, inflection points in amplitude are identified in zero crossings of the first derivative.

Statistical significance of the cross-modality integration effect is determined as follows. First, average waveforms are computed across trials for each subject and electrode independently. Second, FDA is employed to compute the amplitude and derivatives of these waveforms. Third, the inflection points of amplitude as well as derivatives are identified according to zero crossings one derivative above the function of interest. Finally, Student's t-tests (with a Bonferroni correction for multiple electrode sites and $\alpha < 0.05$) are employed to determine if statistically reliable differences in amplitude exist across different experimental conditions; separate analyses are conducted for each electrode. These statistical analyses examine cross-modality integration by using a *maximum criterion* where amplitude in the congruent crossmodal condition has to be significantly greater than both unimodal conditions (auditory and

visual). This maximum criterion is less stringent than a criterion based on super-additivity, where the multisensory condition must be larger than the sum of unisensory responses. In the present study, use of the latter criterion yields no significant effect of integration. Of course, it is not possible to use the above criteria for cross-modality integration to unambiguously identify particular neural or cognitive processes with which they may be associated.

One potential drawback of the proposed approach is that different inflection points may have different latencies; that is, they may not perfectly overlap in time. However, one advantage is that it enables an alignment of inflections across different conditions, therefore factoring out the impact of different temporal latencies, which can be treated as a separate variable.

In order to estimate the topographical distribution of cross-modality integration based on the scalp regions that show a significant effect, the FMRIB Software Library is employed (release 3.2 beta, publicly available at eeg.sourceforge.net) to interpolate continuously between electrode sites.

Based on this interpolation, it is possible to compute the total scalp area spanned in a particular experimental condition. For instance, to examine the effect of cross-modality integration, a binary vector is generated with one value per electrode site, where a value of "1" indicates a significant effect, and "0" indicates no effect. This vector is then processed by the FMRIB software, which returns a topographic map of all sites where significance is met, plus an interpolation between sites. The number of pixels of this activation map is counted and the resulting value is used as a measure of total area size spanned by a particular experimental condition.

Results

Congruent Crossmodal Information Leads to More Accurate and Faster Responses than Incongruent Information

Differences in response times and accuracy are found across experimental conditions, as revealed by one-way analyses of variance (repeated measures ANOVAs with Greenhouse-Geisser correction, followed by analyses of simple effects with significance level of α=.005) with four within-subject levels corresponding to the experimental conditions (auditory, visual, congruent crossmodal, and incongruent crossmodal). Separate analyses are conducted for mean reaction time (RT) and percent correct responses (Fig. 1).

Main effects of condition are found for both RT [$F(3,13)$= 20.6, $p<0.001$] and accuracy [$F(3,13)=27.4$, $p<0.007$]. For both these measures, the congruent crossmodal condition yields an increased performance compared to the incongruent condition; it reaches a higher mean accuracy, while maintaining a lower mean RT. The congruent condition also yields significantly higher accuracy than either auditory or visual conditions, and shorter RTs than the auditory (but not visual) condition. Overall, these results show shorter RTs and higher accuracy for crossmodal stimuli when compared to unimodal stimuli, but only when crossmodal stimuli are congruent (i.e., consistent with the same behavioral response).

Cross-Modality Integration in Higher Derivatives of ERP Waveforms

All electrophysiological results presented here are based on FDA which involves first smoothing the averaged waveforms through B-splines, then computing derivatives. For an example of smoothing for three electrode sites of a single subject, see Fig. 2.; results of all electrode sites for the first, second, and third derivatives (across all subjects) are reported in Supplementary Material Fig. S2–S4. Throughout, the effect of cross-modality integration is assessed using the maximum criterion (i.e., crossmodal amplitude must be larger than the amplitude of both unimodal conditions; see Methods for further details).

To begin investigating cross-modality integration across different derivatives of responses, three electrodes with either an overall strong response to the stimuli (Cz and Pz), or a much weaker one (T5) are examined (Fig. 3). At Cz, a

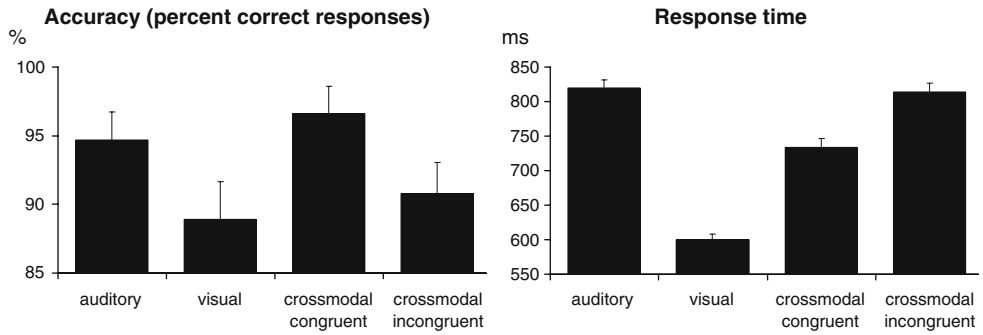

Fig. 1 Crossmodal information and congruency influence the accuracy and reaction times of behavioral responses. Four experimental conditions are displayed: two unimodal (auditory and visual), and two crossmodal (congruent and incongruent). *Vertical bars* represent standard error about the mean

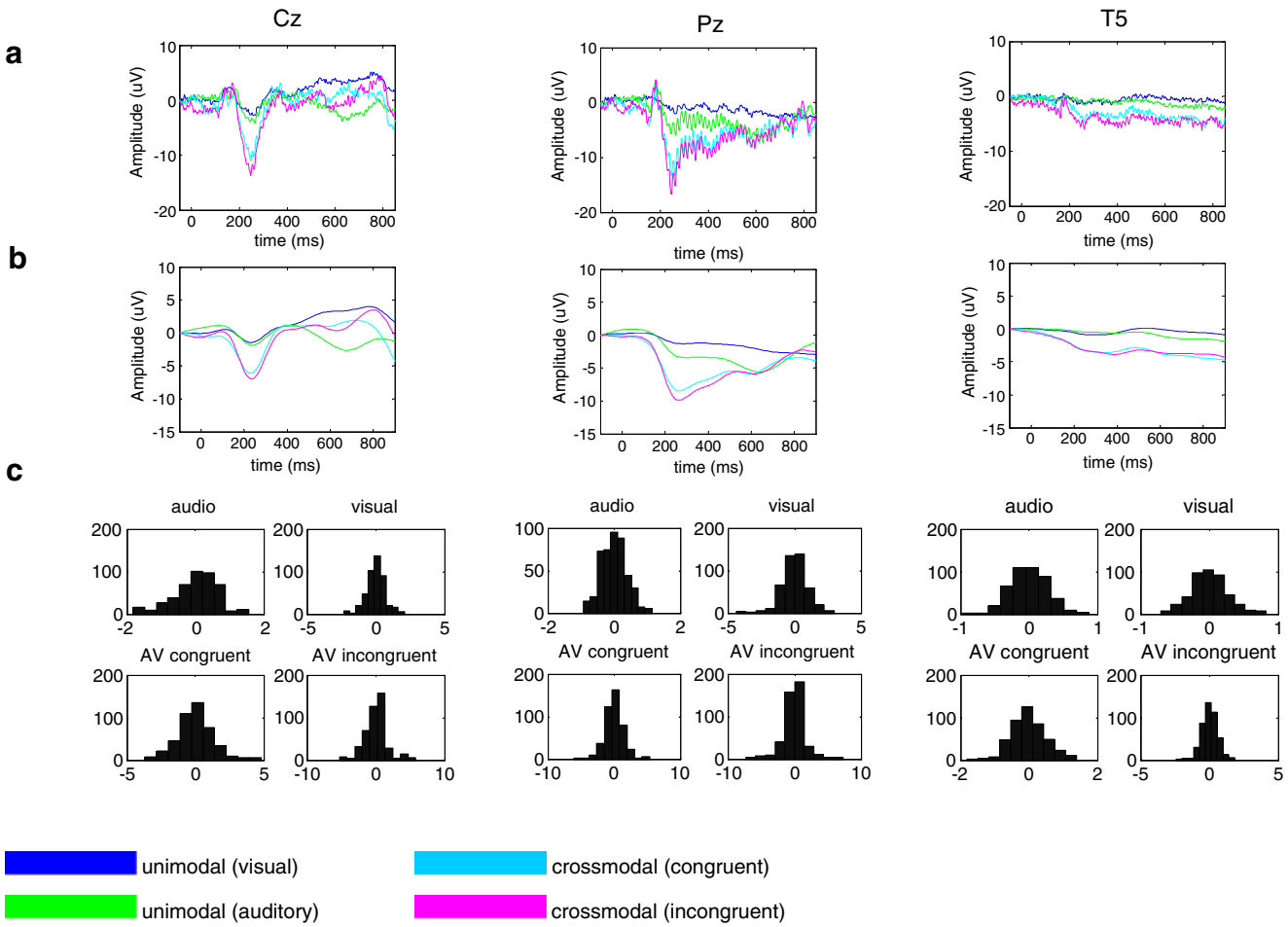

Fig. 2 Example of responses across three electrode sites of a single subject for both unimodal and crossmodal stimuli. **a** Raw waveforms averaged over trials, between −100 and 900 ms with respect to stimulus onset. The four experimental conditions are represented by *different colors* on the figures (see legend). **b** Smoothed waveforms obtained by FDA. **c** Residuals of the least-mean squares fit using FDA (AV=crossmodal condition). These distributions are all approximately Gaussian with a mean of zero and finite variance, therefore meeting the basic requirements for performing FDA

significant effect of cross-modality integration is observed in the positive inflection point of the waveform amplitude around 200 ms post-stimulus onset (Fig. 3, first row, indicated by the asterisk). This effect indicates that activation in the crossmodal congruent condition attains a higher amplitude than both unimodal conditions (visual and auditory). A similar effect is also observed in the first derivative of response (Fig. 3, second row), indicating a sharp rise in activity around 200 ms post-stimulus onset. In the second derivative, both positive (150 ms) and negative (250 ms) inflections yield a significant effect of cross-modality integration (Fig. 3, third row). Finally, a significant effect of cross-modality integration is found in the negative inflection of the third derivative (Fig. 3, fourth row, around 200 ms).

An examination of other sites reveals different signatures of response to cross-modality information. At site Pz, for instance, no effect of cross-modality integration is found for the amplitude of waveforms (Fig. 3, first row). However, a strong effect is found for the positive inflection of the first derivative (Fig. 3, second row, around 200 ms), as is found for Cz. In addition, a significant effect of cross-modality integration is also found in the second derivative of Pz for both positive and negative inflections (Fig. 3, third row), again as found for Cz. No significant effect is found for the third derivative of Pz.

The modulations in amplitude observed at Cz and Pz as a function of cross-modality integration are not observed at every site recorded. For instance, at site T5, only a weak response is found to unimodal and crossmodal stimuli in waveform amplitude as well as in higher derivatives. No significant effect of cross-modality integration is observed.

The above results make clear that the effect of cross-modality integration varies depending on the particular derivative of the ERP waveform considered as well as the recording site. While an effect of cross-modality is observed at Cz and Pz in the early stages of processing (<400 ms post-stimulus onset), it never emerges at T5,

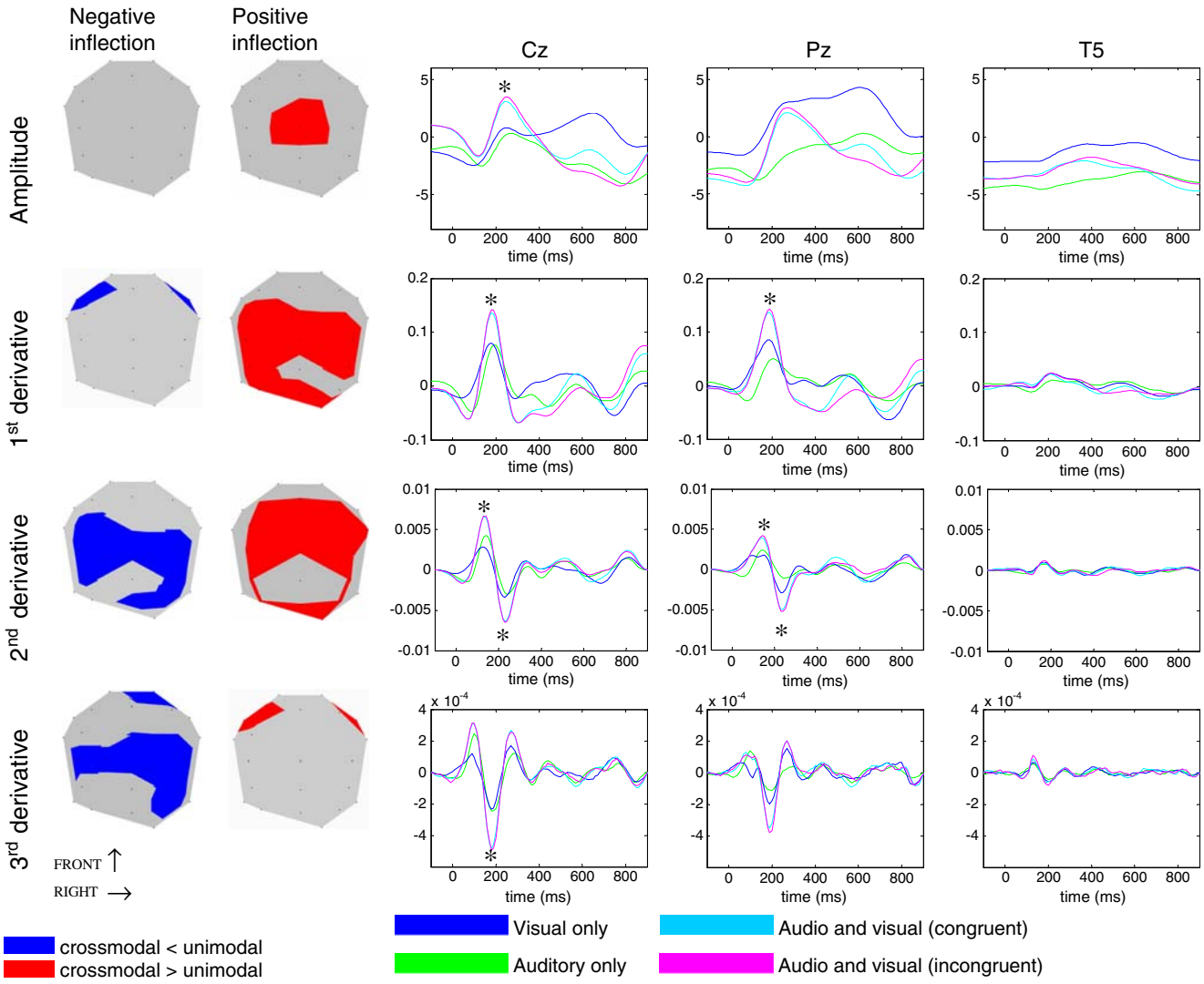

Fig. 3 Topographic distribution of the cross-modality integration effect. The *two left-most columns* show the topographical distribution of scalp regions where a statistically significant effect of cross-modality integration is found (see "Methods"). Both lower inflection points (around 100 ms post-stimulus onset) and higher inflection points (around 200 ms) are reported. The *three right-most columns* show three representative electrode sites (Cz, Pz, and T5). Different rows report the amplitude, first, second, and third derivatives for these sites across the different crossmodal (congruent vs incongruent) and unimodal (auditory vs visual) conditions. Waveforms are averaged across subjects and electrodes. *Asterisks* indicate statistically significant peaks in the waveforms

where all derivatives remain flat for both crossmodal and unimodal stimuli.

The Topographical Distribution of Cross-Modality Integration Varies in Different Derivatives of Responses

To gain more in-depth insights into the spatial distribution of cross-modality integration, topographic maps are computed to identify the areas yielding a significant effect of cross-modality summation (according to a test of maximum criterion, see "Methods"; see Supplementary Material for all topographic distributions across conditions and derivatives). Two sets of analyses are performed, considering either the negative inflection point of waveforms (around 100 ms post-stimulus onset), or the positive inflection point (around 200 ms).

Results show that different derivatives of response—involving the first, second, and third derivatives—yield distinct topographic areas associated with cross-modality integration (Fig. 3, first and second columns). For the amplitude of waveforms, cross-modality integration yields a strong positive inflection associated with a central topography (Cz). For the first derivative of waveforms, this topography broadens to include a wide fronto-centro-parietal distribution (Cz, C3, C4, Pz, P3, CP3, CP4, FC3), as well as one occipital site (O2). The first derivative of waveforms also reveals frontal sites (F3, F7, F8) where crossmodal integration is associated with a negative inflection.

A similar fronto-centro-parietal distribution is observed for both the positive (Fz, F3, F4, Cz, C3, C4, Pz, P3, P4, O2, FT8, CP3, CP3, FC3) and negative (FP1, FP2, Cz, C3, C4, Pz, P4, CP3, CP4, FC3) inflections of the second derivative. A subset of these sites is active for the negative (FP2, Pz, C3, C4, P4, CP4) and positive (FP2, F3, FC3) inflections of the third derivative.

In sum, the topographic distribution of first, second, and third derivatives overlap only partially; each inflection point of each derivative covers a topographic area that is not replicated exactly by any other derivative. Furthermore, the total scalp surface exhibiting cross-modality integration differs according to the particular derivative considered (Fig. 4a), with the first and second derivatives spanning the largest scalp areas. The direction of inflection also influences total scalp surface, with the positive inflection yielding a larger area for both first and second derivatives.

The above results, showing a larger distribution of responses for the first and second derivatives compared to amplitude, are arguably not due to higher derivatives somehow leading to a less stringent criterion for statistical significance. Were this the case, a large scalp area would also be observed for the third derivative, whereas in fact the opposite effect is seen (i.e., the third derivative spans a narrower scalp area than the second derivative for both positive and negative inflections). More elaborate mathematical arguments on this point are available elsewhere (Ramsay and Silverman 2005).

In addition to occupying distinct scalp regions, different derivatives of ERPs display differences in time-course (Fig. 4b). Differences between the temporal distributions of positive and negative inflections are assessed using Student's *t* tests (with Bonferroni correction for multiple derivatives). Significant differences ($p<0.05$) are found between timing of positive and negative inflections for unimodal auditory (all derivatives), unimodal visual (first and second derivatives), crossmodal congruent (first and second derivatives), and crossmodal incongruent stimuli (first and second derivatives). For the first derivative of waveforms, the negative inflection precedes the positive inflection. A different result is obtained for the second derivative: the rate at which the second derivative reaches a peak leads to a sharp positive

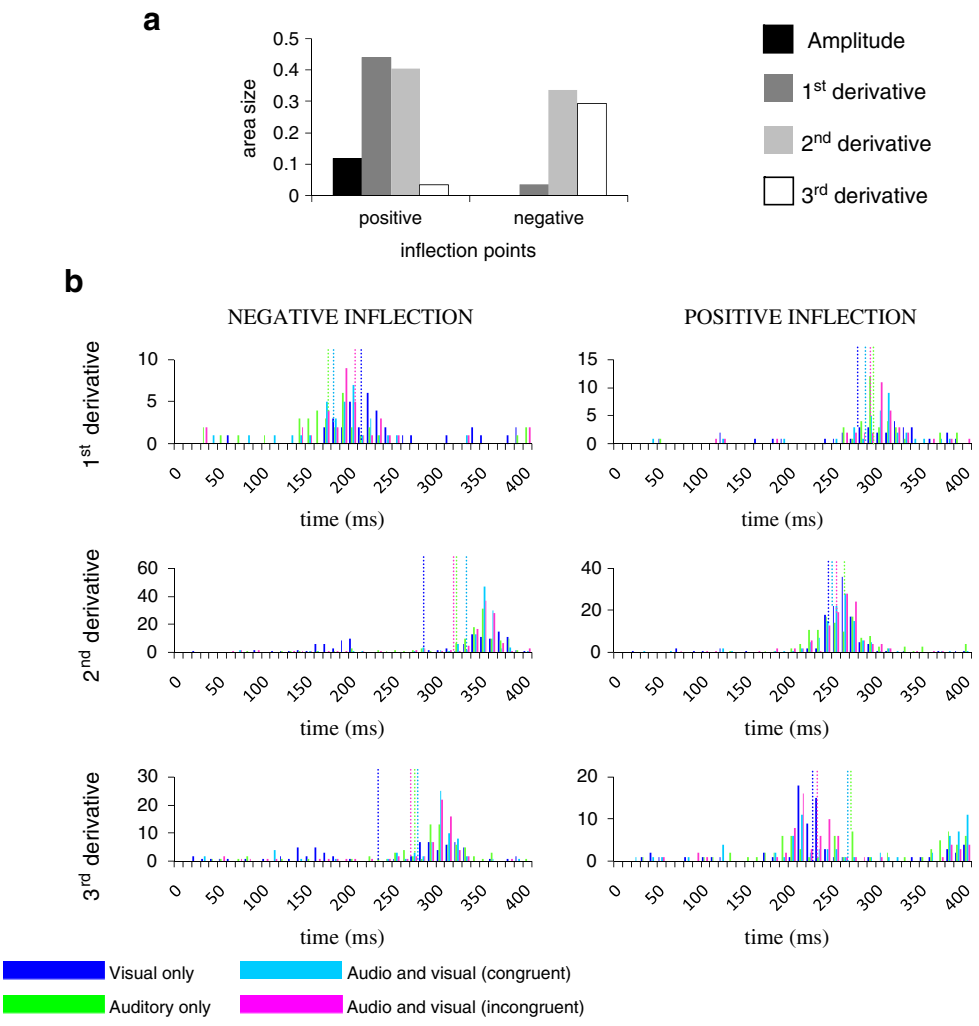

Fig. 4 Scalp areas and temporal latencies associated with different derivatives of waveforms. **a** Total topographical area spanned by different derivatives where significant effects of cross-modality integration are found (see Fig. 3 for scalp distributions). **b** Histograms of temporal latencies for the positive and negative inflection points of different derivatives. *Dashed vertical lines* indicate averages of the different conditions

inflection in amplitude, followed later on by a sharp negative inflection. Similar results are obtained for the third derivative.

Congruency Effects are Found in the First Derivative but Not Amplitude or Higher Derivatives

Do congruent and incongruent crossmodal stimuli influence brain activity in different ways? Are there differences across derivatives of waveforms in the way congruency is processed?

To answer these questions, a first set of analyses is performed with the aim of assessing if there are differences between congruent and incongruent crossmodal conditions prior to 400 ms post stimulus onset (at both negative and positive inflections). This is determined by first identifying points of inflection for both the crossmodal congruent and incongruent conditions, then using Student's *t* tests (with Bonferroni correction for multiple electrodes) to identify topographical sites where these two conditions differ significantly.

Early (<400 ms post-stimulus onset) differences between congruent and incongruent stimuli are found at the negative inflection of the first derivative of waveforms at site F7 (Fig. 5). This result is not obtained with any of the higher derivatives nor in the amplitude of waveforms.

While the above analysis examines congruency effects prior to 400 ms, a second set of analyses is designed to investigate possible effects of congruency occurring after 400 ms (Fig. 6). A more negative-going incongruent response is found in centro-parietal areas (Cz and CPz, first derivative), consistent with previous results (Molholm et al. 2004). A similar centro-parietal network is also activated in positive-going congruent responses (Cz, first derivative; Cz, C4, CPz, and CP4, second derivative). This network is accompanied by activation in frontal areas, yielding both a positive-going incongruent response (F3, amplitude), and a positive-going congruent response (F3, second derivative). No significant differences are found between the timing of positive and negative inflections, nor between the timing of congruent and incongruent conditions. Finally, no sites attained significance for the third derivative.

In sum, despite notable differences across different derivatives of responses, integration and congruency effects activate overlapping scalp areas, consisting primarily of a fronto-centro-parietal distribution. Overall, different regions within this distribution become active early (<400 ms post-stimulus onset) in the case of integration, and later (>400 ms) in the case of congruency.

Discussion

This study compares ERP responses to unimodal and crossmodal stimuli in terms not only of their amplitude, but also higher derivatives (second, third, and fourth). Our hypothesis that different derivatives of response convey information that is not readily accessible from the ampli-

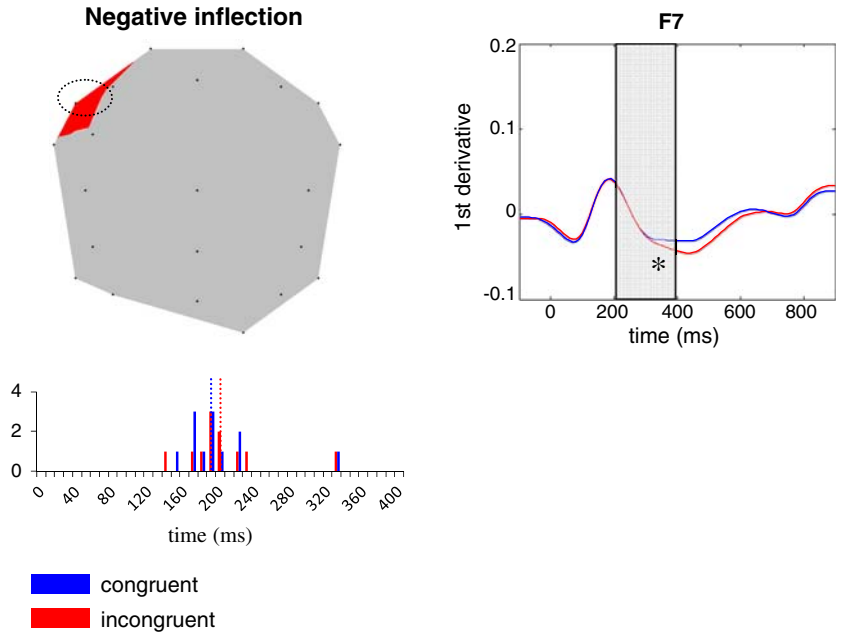

Fig. 5 The congruency of crossmodal information influences the negative inflection of waveforms before 400 ms. *Top left portion of the figure* shows topographical distribution where a significant effect of congruency is found (see "Methods"). The *region in red* has a higher first derivative for incongruent stimuli. *Bottom* Temporal latencies of negative inflection points for the first derivative. *Dashed vertical lines* indicate averages of congruent and incongruent stimuli. *Right* Average waveforms (over subjects and electrodes) for site F7 (topographical location shown by ellipse in *top left figure*), where a significant effect of congruency is found (as indicated by the *asterisk*). *Shaded region* shows time window where congruent and incongruent waveforms begin to diverge

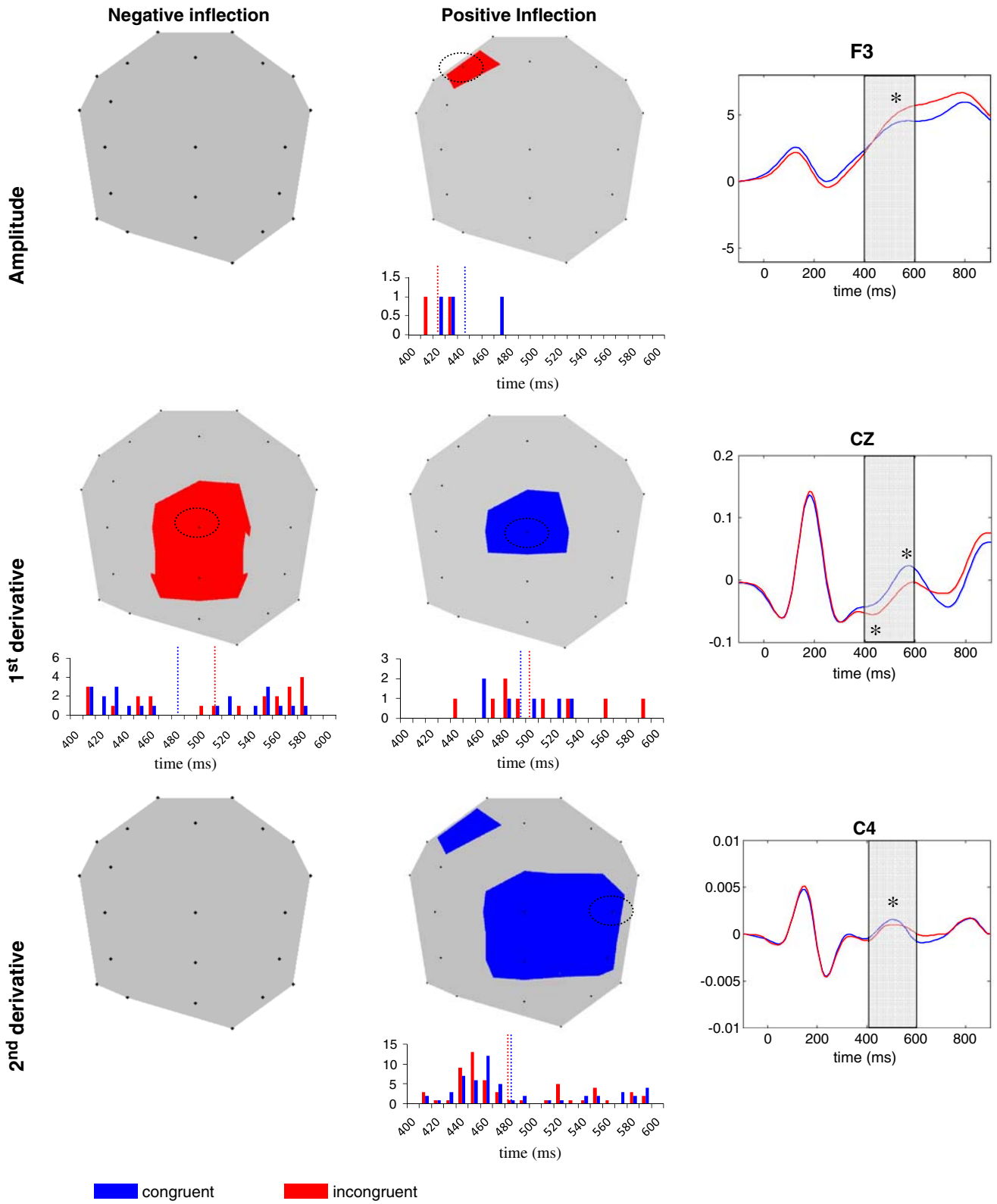

Fig. 6 Congruency influences both amplitude and higher derivatives past 400 ms. *Left and middle columns* show topographical distribution of scalp sites where a significant effect of congruency is found past 400 ms after stimulus onset for positive and negative inflections (see "Methods"). Temporal latencies are plotted below each topographical distribution. *Rightmost column* shows representative waveforms for different sites (topographical locations shown by ellipse in corresponding *top left figure*)

tude of response is largely confirmed. For a number of electrode sites (e.g., Fig. 3, site Pz), cross-modality integration is manifested not in the amplitude of responses, but rather in their first and second derivative. In other words, cross-modality integration is sometimes manifested in a sharper change in activity in response to crossmodal stimuli when compared with unimodal stimuli, and not in a higher amplitude of response.

First and foremost, these results suggest that information may be extracted from analyses of higher derivatives of ERP responses; for instance, examining the second derivative of responses reveals aspects of neural processing that are not accessible to analyses of response amplitudes. When differences are detected between crossmodal and unimodal stimuli, results are always in the same direction, yielding a stronger second derivative to crossmodal stimuli.

Furthermore, our analyses reveal distinct topographic distributions associated with different derivatives of response. A salient example is the significant integration effect for negative inflection points over frontal sites (F3, F7, and F8), a finding that is unique to the first derivative, and was not replicated in analyses of amplitude or other derivatives. This finding suggests that different sites respond to crossmodal stimuli in distinct ways by modulating not the amplitude of their activation, but the speed with which this activation changes over time.

The particular topography of responses associated with congruent and incongruent stimuli depends on the particular time-window considered: while earlier responses (<400 ms) are restricted to frontal regions (F7), later responses (>400 ms) expand to a wider network including frontal, central, and parietal sites. These later responses elicit a stronger (i.e., more positive-going) frontal activation in the amplitude of waveforms for incongruent compared to congruent stimuli (Figs. 5 and 6). These results corroborate previous ERP findings (Molholm et al. 2004) as well as a recent fMRI study showing incongruency-based activation in a fronto-parietal network (including lateral prefrontal cortex and left angular gyrus; Noppeney et al. 2007). In addition, these results may be accommodated by a predictive coding framework (Friston 2005), whereby discrepancies between the representations of top–down and bottom–up streams of information generate an increased cortical response; in the current study, this discrepancy originates from the mismatch between auditory and visual information.

In the derivative of responses, however, results differ from those of waveform amplitudes: congruent stimuli generate positive-going responses (first and second derivatives), while incongruent stimuli generate negative-going responses (first derivative). Overall, these results suggest a potential for two complementary forms of neural codes, by carrying information relevant to incongruency in the positive-going responses of amplitude, and information relevant to congruency in the positive-going responses of derivatives. At the current time, these results must be interpreted with caution, and any conclusion remains to be confirmed by further experiments.

The use of derivatives in the current work is purely for statistical purposes, with no intent of revealing the precise underlying neural correlates of information processing. Nonetheless, it is possible to speculate on the possible neural bases of derivatives. On our account, the sharp second derivative resulting from cross-modality stimuli is compatible with the idea that neurons may rely on different strategies for processing sensory information (Lu and Wang 2004); while some of these strategies may be examined through differences in the amplitude of ERP responses, others may be best examined in higher derivatives. A wealth of data at the cellular level already corroborates this idea. For instance, recent work demonstrates how a simple mechanism based on spike-frequency adaptation may enable neurons to encode the temporal derivative of their firing rate, and reproduce key aspects of motion perception (Puccini et al. 2007). By responding to first-order changes in presynaptic activity, neurons may anticipate changes in presynaptic activation, thus providing a form of predictive coding (Renart et al. 2003). Neural coding based on higher derivatives is also reported in sensory receptors of the vestibular system (Holstein et al. 2004), where it is argued to form the neural substrate for representing Newtonian laws of motion (Angelaki et al. 2004; Shaikh et al. 2005).

While it may seem conceptually difficult to apply similar ideas to second (and higher) derivatives, it is nonetheless conceivable in the following way: neurons sensitive to the rate of change of the above-described neurons (sensitive to first-order changes) would in fact encode second order derivatives. Even though the idea of second-order encoding remains speculative at the present time, and acknowledging that EEG may only reflect weak correlates of cellular mechanisms, it is clear from the present study that higher derivatives of ERP responses carry information that is not found in amplitude alone, and yet exhibit a high degree of statistical reliability with respect to cross-modality integration. Given that time derivatives are argued to form a "fundamental operation in biological circuits" (Puccini et al. 2007), it is perhaps not entirely surprising to find that they possess unique spatiotemporal characteristics reflecting sensory information processing. While there is no straightforward way to relate single cell recordings to measures of scalp activity, our main finding that derivatives of ERPs can convey information adds further weight to the proposal that coding by temporal derivative may form a ubiquitous mode of neuronal communication.

Of course, the proposal of derivative coding cannot be confirmed by the present study based on EEG measures, and several alternative explanations are possible. For instance,

stronger responses to crossmodal stimuli in the first derivative of waveforms may reflect the rapidity at which neural resources are mobilized in order to process sensory information; in short, the more incoming information, the more resources are required for processing and the stronger the first derivative of waveforms. Another possible explanation is that of a high-pass filter: because an inflection point in the derivative of a waveform is indicative of a high frequency in the signal, it is impossible from the analyses performed to discriminate derivative coding from a coding based on band filtering (Andrea Green, personal communication).

At present, novel techniques are being developed to analyze functional connectivity among brain regions involved in particular cognitive functions (e.g., episodic memory; Iidaka et al. 2006). Based on our results showing different distributions of responses for distinct derivatives of ERPs, it is easy to conceive that functional connectivity may change if one considers different derivatives of responses: the temporal correlations that emerge in the amplitude of response of different brain regions may differ markedly from the correlations that emerge in higher derivatives. Two regions whose higher derivatives of response are temporally correlated may form a functional network that is distinct (albeit overlapping) with a functional network of response amplitude. Future studies will be aimed at testing this idea by comparing the functional networks obtained from different derivatives of responses.

Information Sharing Statement

All Matlab software employed in this paper is available online free of charge. The Functional Data Analysis code is available from Jim Ramsay's website: http://www.psych.mcgill.ca/faculty/ramsay/ramsay.html. Tools for the extrapolation of ERP topographical data are available from the FMRIB package: eeg.sourceforge.net. Scripts for data importation of EEG datasets are available from the author by request: jthivier@indiana.edu.

Acknowledgements This work was supported by a Postdoctoral Fellowship from the Fonds Québéçois de Recherche sur les Natures et Technologies (FQRNT). This work benefited from discussions with Jim Ramsay, Thomas Shultz and Frédéric Dandurand (McGill University), as well as data from Natalie Phillips and Axel Winneke (Concordia University).

References

Angelaki, D. E., Shaikh, A. G., Green, A. M., & Dickman, J. D. (2004). Neurons compute internal models of the physical laws of motion. *Nature*, *430*(6999), 560–564.

Basar, E., Demiralp, T., Schurmann, M., Basar-Eroglu, C., & Ademoglu, A. (1999). Oscillatory brain dynamics, wavelet analysis, and cognition. *Brain and Language*, *66*(1), 146–183.

Boersma, P., & Weenink, D. (2006). Praat: doing phonetics by computer (Version 4.5.04): http://www.praat.org.

Demiralp, T., Ademoglu, A., Istefanopulos, Y., Basar-Eroglu, C., & Basar, E. (2001). Wavelet analysis of oddball P300. *International Journal of Psychophysiology*, *39*(2–3), 221–227.

Fort, A., Delpuech, C., Pernier, J., & Giard, M. H. (2002). Early auditory-visual interactions in human cortex during nonredundant target identification. *Cognitive Brain Research*, *14*(1), 20–30.

Freeman, W. J., Holmes, M. D., West, G. A., & Vanhatalo, S. (2006). Fine spatiotemporal structure of phase in human intracranial EEG. *Clinical Neurophysiology*, *117*(6), 1228–1243.

Friston, K. (2005). A theory of cortical responses. *Philosophical Transactions of the Royal Society of London. Series B, Biological Sciences*, *360*(1456), 815–836.

Friston, K., Henson, R., Phillips, C., & Mattout, J. (2006). Bayesian estimation of evoked and induced responses. *Human Brain Mapping*, *27*(9), 722–735.

Giard, M. H., & Peronnet, F. (1999). Auditory-visual integration during multimodal object recognition in humans: a behavioral and electrophysiological study. *Journal of Cognitive Neuroscience*, *11*(5), 473–490.

Gibbons, H., & Stahl, J. (2007). Response-time corrected averaging of event-related potentials. *Clinical Neurophysiology*, *118*(1), 197–208.

Green, P. J., & Silverman, B. W. (1994). *Nonparametric regression and generalized linear models: a roughness penalty approach*. London: Chapman and Hall.

Holstein, G. R., Rabbitt, R. D., Martinelli, G. P., Friedrich, V. L., Jr., Boyle, R. D., & Highstein, S. M. (2004). Convergence of excitatory and inhibitory hair cell transmitters shapes vestibular afferent responses. *Proceedings of the National Academy of Sciences of the United States of America*, *101*(44), 15766–15771.

Iidaka, T., Matsumoto, A., Nogawa, J., Yamamoto, Y., & Sadato, N. (2006). Frontoparietal network involved in successful retrieval from episodic memory. Spatial and temporal analyses using fMRI and ERP. *Cerebral Cortex*, *16*(9), 1349–1360.

Lopes da Silva, F. (1999). Event-related potentials: methodology and quantification. In E. Neidermeyer & F. Lopes da Silva (Eds.), *Electroencephalography*(4th ed.). Philadelphia: Lippincott Williams & Wilkins.

Lu, T., & Wang, X. (2004). Information content of auditory cortical responses to time-varying acoustic stimuli. *Journal of Neurophysiology*, *91*(1), 301–313.

Molholm, S., Ritter, W., Javitt, D. C., & Foxe, J. J. (2004). Multisensory visual-auditory object recognition in humans: a high-density electrical mapping study. *Cerebral Cortex*, *14*(4), 452–465.

Noppeney, U., Josephs, O., Hocking, J., Price, C. J., & Friston, K. J. (2007). The Effect of Prior Visual Information on Recognition of Speech and Sounds. *Cerebral Cortex* (in press).

Picton, T. (1988). *Handbook of electroencephalography and clinical neurophysiology*. Amsterdam: Elsevier.

Puccini, G. D., Sanchez-Vives, M. V., & Compte, A. (2007). Integrated mechanisms of anticipation and rate-of-change computations in cortical circuits. *PLoS Computational Biology*, *3*(5), e82.

Ramsay, J., & Silverman, B. W. (2005). *Functional data analysis, Second edition*. New York: Springer.

Renart, A., Song, P., & Wang, X. J. (2003). Robust spatial working memory through homeostatic synaptic scaling in heterogeneous cortical networks. *Neuron*, *38*(3), 473–485.

Shaikh, A. G., Green, A. M., Ghasia, F. F., Newlands, S. D., Dickman, J. D., & Angelaki, D. E. (2005). Sensory convergence solves a motion ambiguity problem. *Current Biology*, *15*(18), 1657–1662.

Teder-Salejarvi, W. A., Di Russo, F., McDonald, J. J., & Hillyard, S. A. (2005). Effects of spatial congruity on audio-visual multimodal integration. *Journal of Cognitive Neuroscience*, *17*(9), 1396–1409.

Thivierge, J. (2007). Functional data analysis of cognitive events in EEG. Paper presented at the IEEE International Conference on Systems, Man, and Cybernetics, Montreal, Canada.